Surface tension of chain molecules through a combination of the gradient theory with the CPA EoS

M.B. Oliveira[a], I.M. Marrucho[a], J.A.P. Coutinho[a], A.J. Queimada[b],*

[a] CICECO, Chemistry Department, University of Aveiro, 3810-193 Aveiro, Portugal
[b] LSRE - Laboratory of Separation and Reaction Engineering, Faculdade de Engenharia, Universidade do Porto, Rua do Doutor Roberto Frias, 4200 - 465 Porto, Portugal

ARTICLE INFO

ABSTRACT

Despite the interest in systems containing non-associating compounds such as alkanes and fluoroalkanes or associating compounds like alkanols, their vapor–liquid interfaces have received little quantitative attention. Aiming at modeling the interfacial tensions of several families of chain molecules, a combination of the density gradient theory of fluid interfaces with the Cubic-Plus-Association (CPA) equation of state was developed. The density gradient theory is based on the phase equilibria of the fluid phases separated by the interface, for what an adequate equation of state is required.

In this work, the series of the n-alkanes, n-perfluoroalkanes and n-alkanols were studied in a broad temperature range. It will be shown that even for non-associating compounds such as the n-alkanes, CPA can improve considerably the estimation of vapor pressures and coexisting phase densities, which are important for the accuracy of the surface tensions obtained through the density gradient theory. The surface tensions of the compounds studied were accurately described with a global average deviation of 0.5%.

As it will be shown, the combination of the density gradient theory with the CPA EoS also allowed very good predictions of the surface tensions of some binary mixtures.

A discussion on the regression and selection of pure component parameters is also reported.

© 2008 Elsevier B.V. All rights reserved.

1. Introduction

Interfacial tension controls many processes in chemical and reservoir engineering applications. For instance, in the petroleum industry, very low surface tensions are involved in operations where liquid and vapor phases are present in reservoirs, such as during secondary and tertiary oil recovery [1]. As a result, surface tensions are required to be precisely known since they strongly influence the capillary pressure, relative permeabilities and the residual liquid saturation.

Other processes that have a strong dependence on the surface tensions are, for example, the adhesion of thin films over surfaces [2], the stability of foams [3], the generation of bubbles and drops [4], the production of some foods and drugs [5], the phase behavior in porous media and processes of simultaneous mass and heat transfer [6]. Surface tension also interferes on the quality of products like paints, coatings, anticorrosives, agrochemicals and detergents.

New legislation and restrictions on the hydrocarbon content of aqueous effluents require these pollutants to be removed from refinery and petrochemical plant wastewater streams. The knowledge of interfacial tension helps to determinate the path, transport and fate mechanisms of these organic pollutants in the environment.

Although large attention has been given to the measurement and modeling of phase equilibria, little work was done before on interfacial properties such as surface tensions. Experimental measurements are expensive and time consuming and the different conditions of temperature, pressure and composition that may be of interest suggests the development of theoretical tools, assessed against an evaluating database, that can latter be used to correlate or predict surface tensions in a broad range of conditions.

There are many approaches for computing the surface tensions of simple fluids and mixtures. The most basic approach is the parachor method [7] and its derivatives. The corresponding-states principle [8–11] and other thermodynamic correlations [12–14] are alternative approaches to the description of surface/interfacial

tensions. Some more complex theories also take into account the density gradients in the interface like the perturbation theory [15], integral and density functional theories [16–19], or the gradient theory of fluid interfaces [20,21]. A generalized version of a corresponding states model for pure fluids and mixtures had also been developed, using a simple cubic EoS as a reference EoS, allowing an excellent representation of the surface tension of several pure alkanes and their mixtures with water [22]. Panayiotou [23] extended the QCHB equation-of-state model to interfaces obtaining a satisfactory agreement between experimental and calculated surface tensions of pure fluids. The density functional theory (DFT) can also be used for the prediction of surface tensions [24].

The gradient theory of fluid interfaces has its origin in the work of van der Waals [20] and was reformulated by Cahn and Hilliard [21]. This theory converts statistical mechanics of inhomogeneous fluids into a non-linear boundary value problems that can be solved to compute the density and the stress distributions in the interface. In the reformulation made by Cahn and Hilliard the surface tension can be calculated by a theory that describes a continuous evolution of the Helmholtz energy along the interface. The physical consistency of this approach was confirmed by the regular solution theory for qualitatively describing the properties of planar interfaces [21]. Consequently, one of the gradient theory inputs is the Helmhotz free energy density that can be computed by any thermodynamic model, like an equation of state. The likely advantage of this approach is that simultaneous modeling of interfacial tensions and phase equilibria is possible.

Accurate estimates of surface tensions for short-chain, nonpolar fluids were previously achieved through standard cubic EoSs with quadratic mixing rules. The Peng-Robinson EoS and the SRK EoS were used with success to describe the interfacial properties of simple mixtures containing just hydrocarbons [25–30]. Some problems related with the well known deficiencies of cubic EoS for describing the liquid phase densities of longer chain molecules where corrected by Miqueu et al. using a volume translation [28,31,32]. However, unphysical results are still obtained for systems containing polar and/or associating compounds [33]. For these systems it is necessary to either employ advanced mixing rules, such as the Wong-Sandler or the modified Huron-Vidal mixing rules, as previously done by Mejia et al. [34,35] or, instead, use a model explicitly incorporating association due to hydrogen bonding and anisotropic interactions. For that purpose, Cornelisse et al. combined the gradient theory with the Associated-Perturbed-Anisotropic-Chain Theory (APACT) and the interfacial tensions computed agreed well with experiments for systems composed of n-alkanols and water [36].

Panayiotou combined the gradient theory of fluid interfaces with the QCHB (quasi-chemical hydrogen-bonding) equation-of-state model to compute surface tensions. The results obtained were rather satisfactory for pure fluids and for mixtures of non polar or weakly polar fluids, and in qualitative agreement with the experimental data for associating mixtures [23,37].

Another approach to describe interfacial properties of polar mixtures is to use the Statistical Association Fluid Theory (SAFT). The studies performed by Kahl and Enders [33] and more recently by Fu [38] showed that the SAFT EoS for alcohols leads to satisfactory results.

Kahl and Enders [33] demonstrated that the prediction of water surface tension depends on the number of association sites and so, the association model used must be selected very carefully. Significant problems were also detected for polar compounds in the critical region. In addition, it was found that the SAFT-EoS gives at lower temperatures better surface tension modeling results than the APACT-EoS, whereas at higher temperatures, the APACT-EoS is superior to the SAFT-EoS.

A new model in the family of association equations of state such as SAFT and APACT, is the Cubic-Plus-Association (CPA) equation of state. This equation of state combines the Soave-Redlich-Kwong (SRK) cubic equation of state for the physical contribution with the association contribution proposed by Wertheim. The CPA EoS has already shown to be able to satisfactorily model the phase equilibria for water containing systems, with alkanes, cycloalkanes and alkenes [39], aromatics [40], alcohols [41] glycols [42] and fluoroalkanes [43].

In spite of these good results obtained with the CPA EoS for phase equilibria, only Queimada et al. [44] attempted to combine the gradient theory with the CPA EoS to describe hydrocarbon liquid–vapor interfaces, with very good results. In this work, this approach is successfully extended to the modeling of surface tensions of the homologue families of n-alkanes (C_2–C_{36}), n-fluoroalkanes (C_3–C_9) and n-alkanols (C_1–C_{20}), and a systematic investigation of the trends of the parameters as well as of the sensitivity of the results to the influence parameter was performed.

This approach was also extended here to predict vapor–liquid interfacial tensions of five mixtures (methane + pentane, ethane + nonane, methanol + ethanol, octane + heptanol and octane + octanol) with very good results.

2. Model

The gradient theory is based on the phase equilibria of the fluid phases separated by an interface, generalized for multicomponent mixtures by Miqueu et al. [28,32,44,45]:

$$\sigma = \int_{n_N^{vap}}^{n_N^{liq.}} \sqrt{2\Delta\Omega(n)\sum_i\sum_j c_{ij}\frac{dn_i}{dn_N}\frac{dn_j}{dn_N}}\, dn_N \qquad (1)$$

$$\Delta\Omega(n) = \Omega(n) + p \qquad (2)$$

where p is the equilibrium pressure, σ is the interfacial tension, $f_0(n)$ is the Helmholtz free energy density of the homogeneous fluid, at local composition n, μ_i are the pure-component chemical potentials, $n^{liq.}$ and n^{vap} are the liquid and vapor phase densities, subscript N stands for the mixture reference component and c is the so-called influence parameter. $\Omega(n)$ is the grand thermodynamic potential defined as:

$$\Omega(n) = f_0(n) - \sum_i n_i\mu_i \qquad (3)$$

being $f_0(n)$ the Helmholtz free energy density of the homogeneous fluid, at local composition n, and μ_i the pure component chemical potentials.

The pure-component influence parameter, c, has a theoretical definition, but this can hardly be implemented. For practical purposes, after the vapor–liquid equilibrium is determined, this is correlated from surface tension data:

$$c_{ii} = \frac{1}{2}\left[\frac{\sigma_{exp}}{\int_{n^{vap}}^{n^{liq.}}\sqrt{f_0(n) - n\mu + p}\, dn}\right]^2 \qquad (4)$$

For mixtures, cross influence parameters, c_{ij}, are calculated from a combining rule that is reduced to a geometric mean rule whenever the binary interaction coefficients (k_{ij}) are set to zero, making the method predictive:

$$c_{ij} = (1 - k_{ij})\sqrt{c_{ii}c_{jj}} \qquad (5)$$

To use the gradient theory, it is necessary to determine the equilibrium densities of the coexisting phases, the chemical potentials and the Helmholtz free energy using an adequate model. In this work, the CPA equation of state will be used for these purposes.

Table 1
Critical temperatures, CPA parameters and modeling results for *n*-alkanes

Fluid	T_c (K)	a_0 (J m^3 mol^{-2})	c_1	b ($\times 10^5$ m^3 mol^{-1})	%AAD	
					p	$\rho^{liq.}$
C_2H_6	305.3	0.55113	0.58719	4.2967	0.09	1.10
C_3H_8	369.8	0.91666	0.67005	5.8871	0.29	0.81
C_4H_{10}	425.1	1.3464	0.72832	7.4797	0.25	0.68
C_5H_{12}	469.7	1.8233	0.80178	9.1314	0.44	0.58
C_6H_{14}	507.6	2.3396	0.86862	10.802	0.54	0.63
C_7H_{16}	540.2	2.8883	0.93390	12.496	1.17	0.57
C_8H_{18}	568.7	3.4747	1.0041	14.222	1.02	0.67
C_9H_{20}	594.6	4.0960	1.0640	15.992	1.23	0.85
$C_{10}H_{22}$	617.7	4.7583	1.1121	17.772	1.28	1.09
$C_{11}H_{24}$	639	5.4293	1.1747	19.600	1.67	1.27
$C_{12}H_{26}$	658	6.1502	1.2191	21.435	1.62	1.46
$C_{13}H_{28}$	675	6.8993	1.2749	23.382	1.49	1.87
$C_{14}H_{30}$	693	7.6340	1.3166	25.179	1.50	1.80
$C_{15}H_{32}$	708	8.4414	1.3508	27.074	1.02	2.03
$C_{16}H_{34}$	723	9.2020	1.4044	28.964	1.84	2.16
$C_{17}H_{36}$	736	10.053	1.4406	30.862	1.40	2.23
$C_{18}H_{38}$	747	10.856	1.4853	32.730	1.45	2.42
$C_{19}H_{40}$	755	11.654	1.5416	34.521	2.62	2.65
$C_{20}H_{42}$	768	12.583	1.5748	36.627	2.84	2.65
$C_{22}H_{46}$	786	14.365	1.6493	40.540	3.55	2.76
$C_{23}H_{48}$	790	15.477	1.6831	42.653	2.90	3.08
$C_{24}H_{50}$	800	16.554	1.6917	44.821	2.15	3.43
$C_{25}H_{52}$	810.1	17.297	1.7501	46.620	2.68	3.34
$C_{26}H_{54}$	817.1	18.467	1.7652	48.847	1.56	3.67
$C_{27}H_{56}$	823.7	19.423	1.8066	50.590	0.87	3.91
$C_{28}H_{58}$	829.9	20.654	1.8168	53.179	2.24	2.94
$C_{29}H_{60}$	835.7	21.654	1.8462	55.178	3.32	2.64
$C_{30}H_{62}$	841.3	22.794	1.8552	57.134	3.57	2.86
$C_{32}H_{66}$	851.4	25.598	1.8877	62.715	2.14	3.00
$C_{36}H_{74}$	868.8	30.415	1.9321	70.520	3.93	2.93
Average deviation					1.76	2.07

The CPA EoS, in terms of the compressibility factor, can be expressed as the sum of two contributions: one accounting for physical interactions, that in the current work is taken as the SRK EoS, and another accounting for association, the Wertheim association term [39,46–50]:

$$Z = Z^{phys.} + Z^{assoc.} = \frac{1}{1-b\rho} - \frac{a\rho}{RT(1+b\rho)} - \frac{1}{2}\left(1 + \rho\frac{\partial \ln g}{\partial \rho}\right)$$
$$\sum_i x_i \sum_{A_i}(1 - X_{Ai}) \qquad (6)$$

where *a* is the energy parameter, *b* the co-volume parameter, ρ the density, *g* the simplified radial distribution function [48], X_{Ai} the mole fraction of pure component *i* not bonded at site *A* and x_i is the mole fraction of component *i*.

The pure component energy parameter of CPA has a Soave-type reduced temperature (T_r) dependency:

$$a(T) = a_0[1 + c_1(1 - \sqrt{T_r})]^2 \qquad (7)$$

The pure compound parameters (a_0, c_1 and *b*) are regressed from selected pure component vapor pressure and liquid density data.

X_{Ai} is related to the association strength $\Delta^{A_iB_j}$ between two sites belonging to two different molecules and is calculated by solving the following set of equations:

$$X_{Ai} = \frac{1}{1 + \rho \sum_j x_j \sum_{B_j} X_{Bj} \Delta^{A_iB_j}} \qquad (8)$$

Where for self-associating molecules we have:

$$\Delta^{A_iB_i} = g(\rho)\left[\exp\left(\frac{\varepsilon^{A_iB_i}}{RT}\right) - 1\right] b_{ii}\beta^{A_iB_i} \qquad (9)$$

where $\varepsilon^{A_iB_i}$ and $\beta^{A_iB_i}$ are the association energy and the association volume, respectively, and for sites belonging to two different associating molecules, the Elliot's combining rule is used:

$$\Delta^{A_iB_j} = \sqrt{\Delta^{A_iB_i} \times \Delta^{A_jB_j}} \qquad (10)$$

The simplified radial distribution function, $g(\rho)$ is given by [48]:

$$g(\rho) = \frac{1}{1 - 1.9\eta} \quad \text{where} \quad \eta = \frac{1}{4}b\rho \qquad (11)$$

For non-associating components such as *n*-alkanes and *n*-fluoroalkanes CPA has three pure component parameters (a_0, c_1 and *b*) while for associating components like *n*-alkanols it has five (a_0, c_1, *b*, ε and β). In both cases, parameters are regressed simultaneously from vapor pressure and liquid density data.

For *n*-alkanols, the 2B association scheme applies, according to the nomenclature of Huang and Radosz [51], where it was proposed that hydrogen bonding occurs between the hydroxyl hydrogen and one of the lone pairs of electrons from the oxygen atom in another *n*-alkanol molecule:

$$X_A = X_B = \frac{-1 + \sqrt{1 + 4\rho\Delta^{AB}}}{2\rho\Delta^{AB}} \qquad (12)$$

$$\Delta^{AA} = \Delta^{BB} = 0, \qquad \Delta^{AB} \neq 0. \qquad (13)$$

3. Results and discussion

For *n*-alkanes and *n*-fluoroalkanes the CPA EoS reduces to the SRK EoS and has only the three pure component parameters of the physical part. For *n*-alkanols, being associative fluids, two more parameters must be estimated, the association energy and volume. All the pure component parameters were determined by a simultaneous regression of saturated vapor pressure and liquid density

Table 2
Critical temperatures, CPA parameters and modeling results for *n*-alkanols (the 2B scheme applies)

Fluid	T_c (K)	a_0 (J m^3 mol^{-2})	c_1	b ($\times 10^5$ m^3 mol^{-1})	β	ε (J mol^{-1})	%AAD	
							p	$\rho^{liq.}$
CH_3OH	512.7	0.43268	0.74696	3.2151	3.4096E−02	20859	0.29	0.14
C_2H_5OH	514.7	0.68415	0.93923	4.7508	1.9212E−02	21336	0.35	0.51
C_3H_7OH	536.8	1.1424	0.90134	6.3788	7.7360E−03	21913	0.13	0.34
C_4H_9OH	562.9	1.8019	0.98766	8.1309	3.6694E−03	20069	0.40	0.61
$C_5H_{11}0H$	587.7	2.3552	1.0690	9.7179	2.6724E−03	18666	0.30	0.50
$C_6H_{13}OH$	610.7	2.8386	0.96959	11.313	1.6727E−03	22759	0.54	0.75
$C_7H_{15}OH$	632.6	3.5210	1.1282	13.107	2.4419E−04	25202	0.72	0.71
$C_8H_{17}OH$	653.6	4.1507	1.0417	14.813	4.0973E−04	25820	0.51	1.13
$C_9H_{19}OH$	671.8	4.7022	1.2018	16.460	2.4486E−04	25588	1.07	0.62
$C_{10}H_{21}OH$	689.6	5.3432	1.2921	18.274	8.3873E−05	27226	1.17	0.96
$C_{11}H_{23}OH$	696.6	6.0610	1.2155	20.045	3.3535E−04	26496	0.61	1.30
$C_{12}H_{25}OH$	705.1	6.9861	1.2575	22.007	2.5163E−04	26517	1.79	1.51
$C_{13}H_{27}OH$	720	7.9073	1.2451	24.201	1.9469E−04	28148	0.66	2.33
$C_{14}H_{29}OH$	729	8.8411	1.2853	26.132	8.8704E−05	29642	0.55	2.23
$C_{15}H_{31}OH$	745.3	9.6045	1.3096	27.970	1.4118E−04	29306	0.76	2.37
$C_{16}H_{33}OH$	752.8	10.559	1.3487	30.027	8.2959E−05	30718	0.47	2.55
$C_{17}H_{35}OH$	766.1	11.351	1.3667	31.674	9.3611E−05	30297	1.00	2.93
$C_{18}H_{37}OH$	771.7	12.409	1.3728	33.707	8.2914E−05	31362	1.02	2.72
$C_{19}H_{39}OH$	784.4	13.148	1.3992	35.456	7.0136E−05	32082	1.11	3.06
$C_{20}H_{41}OH$	793.7	14.012	1.4094	37.385	7.2628E−05	34091	1.13	3.12
Average deviation							0.73	1.52

data. The required data was collected from the *NIST Chemistry Web-Book* [52] for lighter *n*-alkanes and from the *DIPPR* database [53] for *n*-alkanes and *n*-alkanols. For the heavier *n*-alkanes vapor pressure data was collected from literature [54–57]. For *n*-fluoroalkanes data was collected from literature [58–74]. Results are presented in Table 1 for *n*-alkanes, Table 2 for *n*-alkanols and Table 3 for *n*-fluoroalkanes.
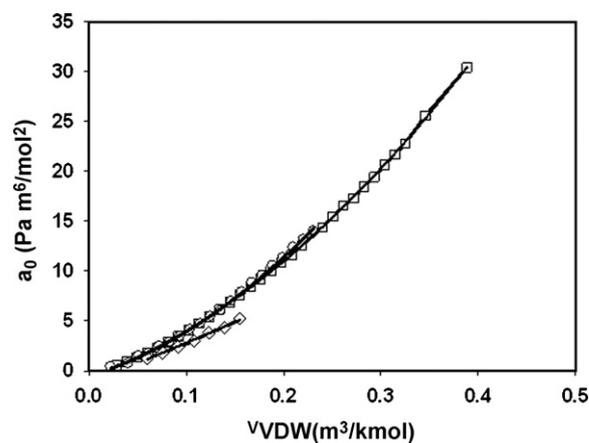
As can be seen from Tables 1–3 very good vapor pressure and liquid density results are obtained from CPA (0.45 < T_r < 0.85 for *n*-alkanes and *n*-alkanols and T_r > 0.43 for fluoroalkanes) using the fitted pure compound parameters. For *n*-alkanes the global average deviations were 2% both for vapor pressure and liquid densities, in the wide range of compounds from C_2 to C_{36}. For *n*-alkanols global average deviations of only 0.7% for the vapor pressure and of 1.5% for the liquid density were achieved for compounds from methanol to *n*-eicosanol. For *n*-fluoroalkanes global average deviations of 2% for vapor pressure and for liquid densities were obtained for the seven compounds studied. On previous works [75–77], the CPA pure compounds parameters of some *n*-alkanes and *n*-alkanols had already been estimated and our values are very similar to those ones.

This better description is achieved by using the fitted *a* and *b* parameters when compared with those obtained using the classical *a* and *b* expressions of SRK. When the classic cubic EoS are employed, such as the PR EoS, good results for the equilibrium liquid phase densities are only possible with the inclusion of a volume correction [28,31,32]. As expected for equations of state, higher deviations are obtained near the critical point [47].

The pure compound parameters of the physical part of CPA for the *n*-alkanes, *n*-alkanols and *n*-fluoroalkanes seem to follow a
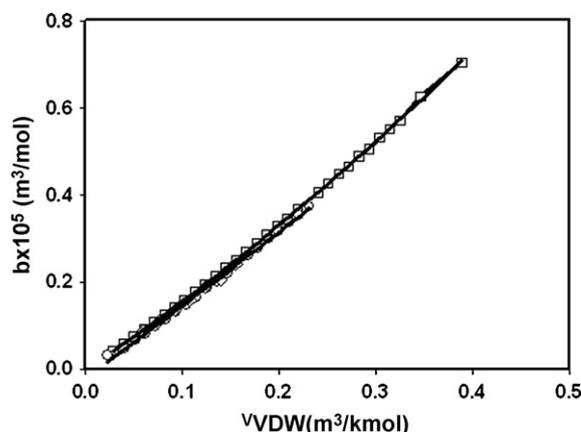

Fig. 1. CPA pure parameter a_0 trend with the van der Waals volume (□, *n*-alkanes; ○, *n*-alkanols; ◇, FCs).

trend within the homologous series, when plotted as a function of the van der Waals volume (Figs. 1 and 2), what allows the CPA EoS to be used as a predictive tool for these families of compounds. Therefore, pure component parameters can be computed for those for

Table 3
Critical temperatures, CPA parameters and modeling results for *n*-fluoroalkanes

Fluid	T_c (K)	a_0 (J m^3 mol^{-2})	c_1	b ($\times 10^5$ m^3 mol^{-1})	%AAD	
					p	$\rho^{liq.}$
C_3F_8	344.9	1.2741	0.90586	8.7408	2.90	2.50
C_4F_{10}	386.4	1.8120	0.96275	11.020	0.80	2.50
C_5F_{12}	421.4	2.4339	1.0428	13.506	2.70	2.00
C_6F_{14}	449	2.9895	1.1991	15.887	5.00	1.90
C_7F_{16}	475.3	3.8246	1.2086	18.942	2.80	2.00
C_8F_{18}	498	4.3690	1.3226	20.592	0.90	3.60
C_9F_{20}	524	5.2330	1.4160	24.189	1.20	2.40
Average deviation					2.33	2.41

Fig. 2. CPA pure parameter *b* trend with the van der Waals volume (□, *n*-alkanes; ○, *n*-alkanols; ◇, FCs).

Table 4
Correlations for the variation of the CPA pure compounds parameters with the van der Waals volume

	a_0	b	c_1	ε	β
n-Alkanes	$110.04 V_{VDW}^2$ $+ 37.56 V_{VDW} - 0.81$	$1.83 \times 10^{-3} V_{VDW}$ $- 3.16 \times 10^{-5}$	$-5.49 V_{VDW}^2$ $+ 5.86 V_{VDW} + 0.52$		
n-Alkanols				$98909 V_{VDW}^2 + 35398 V_{VDW} + 20018$	$1.14 \times 10^{-6} V_{VDW}^{-2.71}$
n-FC	$41.38 V_{VDW} - 1.32$				

which vapor pressure and density data are not available. Quadratic and linear correlations for the variation of these parameters with the van der Waals volume were proposed, as can be seen in Table 4. It is interesting to note that the same trends on each parameter (a_0, c_1 and b) are observed for the three different families. In fact, the regressed values of a_0 for the n-alkanols almost match those of the same chain length n-alkane, being possible to use the same correlation for these two families, and for the fluoroalkanes a simple linear correlation is applied. Moreover, the correlation lines of the three families for b are quite similar to each other, what allows us to correlate a single linear trend to the three families of compounds studied. For c_1 since a similar quadratic trend is observed for the three families, the same correlation can be proposed. The two additional associating CPA parameters for n-alkanols also have a van der Waals volume dependency, as described by the equations in Table 4.

Once the phase equilibria is correctly described, the gradient theory is applied to calculate surface tensions.

As mentioned before, the pure-component influence parameter, c_{ii}, has a theoretical definition, but that can hardly be implemented, since the necessary direct correlation function is not available for most of these systems [45]. For practical purposes the influence parameter, is adjusted from surface tension data and plotted (far from the critical point), using the energy and the co-volume parameters of the physical part of the CPA EoS, as $c/ab^{2/3}$ as a function of $1 - T_r$, as already done in previous works [28,32,44].

In a previous paper, Queimada et al. [44] studied, for n-heptane, the effect of the cubic term on the change of $c/ab^{2/3}$ with reduced temperature. It was found that at $T_r < 0.8$ both SRK, PR and CPA gave similar values, but that at higher temperatures the values from the equations of state whose parameters were calculated from critical properties (SRK and PR) diverged while approaching the critical temperature (as expected from theory), whereas CPA $c/ab^{2/3}$ values converge. As mentioned in that work, this is due to the fact that while using fitted parameters, CPA cannot adequately describe the critical temperature, which is implicit in the calculation of the influence parameters through the dependence of surface tension on temperature (that shall be zero at T_c).

Previous approaches combining the density gradient theory with different versions of the SAFT EoS considered the influence parameter either as temperature independent [33] or temperature dependent [38], while studies with cubic EoS revealed that a linear dependence in reduced temperature would be more adequate [28,32]. A recent work also proposed a correlation for the influence parameter which was generalized as a function of the critical compressibility factor, the acentric factor, the reduced dipole moment and the reduced temperature [78].

With regard to the present work, some of the components presented variations of $c/ab^{2/3}$ that were typically quadratic with $(1 - T_r)$, other linear, and other almost constant, which in some cases can be explained by the limited reduced temperature range

Table 5
Correlations coefficients for calculating the influence parameters, its constant value for $T_r = 0.65$ and modeling results for n-alkanes

Fluid	$D \times 10^{16}$	$E \times 10^{16}$	$F \times 10^{16}$	$c/ab^{2/3} \times 10^{16}$ const	%AAD	
					σ (corr)	σ ($c/ab^{2/3} \times 10^{16}$ const)
C_2H_6	1.0583	−1.2953	0.6875	0.6854	0.10	5.87
C_3H_8	0.9981	−1.1119	0.5462	0.6751	0.09	5.35
C_4H_{10}	0.8280	−0.6986	0.2506	0.6151	0.24	4.29
C_5H_{12}	0.8549	−0.8388	0.2647	0.5962	0.07	5.56
C_6H_{14}	0.6969	−0.4010	−0.0130	0.5549	0.02	3.84
C_7H_{16}	0.6990	−0.4834	0.0865	0.5394	0.04	3.90
C_8H_{18}	0.7244	−0.7020	0.2465	0.5110	0.00	5.23
C_9H_{20}	0.5491	−0.0805	−0.3121	0.4740	0.55	3.16
$C_{10}H_{22}$	0.4931	0.0391	−0.4012	0.4573	0.14	2.66
$C_{11}H_{24}$	0.4364	0.1531	−0.4743	0.4307	0.09	1.97
$C_{12}H_{26}$	0.4052	0.2171	−0.5195	0.4171	0.22	1.61
$C_{13}H_{28}$	0.3852	0.2563	−0.5507	0.4078	0.11	1.59
$C_{14}H_{30}$	0.3204	0.4276	−0.6744	0.3876	0.17	1.37
$C_{15}H_{32}$	0.2946	0.4896	−0.7169	0.3785	0.17	1.39
$C_{16}H_{34}$	0.2147	0.8090	−1.1073	0.3620	0.51	1.82
$C_{17}H_{36}$	0.1882	0.8194	−1.0187	0.3494	0.23	2.06
$C_{18}H_{38}$	0.1921	0.7620	−0.9532	0.3417	0.24	2.07
$C_{19}H_{40}$	0.1643	0.8976	−1.1929	0.3314	0.71	2.44
$C_{20}H_{42}$	0.1474	0.8447	−1.0076	0.3196	0.25	0.00
$C_{22}H_{46}$	0.2490	0.2490	0.2490	0.3457	0.46	1.97
$C_{23}H_{48}$	0.1913	0.7924	−1.0558	0.3391	0.08	2.21
$C_{24}H_{50}$	0.1047	1.0773	−1.3015	0.3212	0.41	3.40
$C_{25}H_{52}$	0.1564	0.7906	−1.0283	0.3071	0.10	0.01
$C_{26}H_{54}$	0.2241	0.5354	−0.7276	0.3220	2.45	3.16
$C_{27}H_{56}$	0.1379	0.8052	−0.9941	0.2983	5.42	0.00
$C_{28}H_{58}$	0.1367	0.8436	−1.0625	0.3020	0.30	3.00
$C_{29}H_{60}$	0.1107	0.8638	−1.0419	0.2862	0.72	4.07
$C_{30}H_{62}$	0.0842	0.9118	−1.0917	0.2695	0.54	4.08
$C_{32}H_{66}$	0.2266	0.4222	−0.6523	0.2947	0.59	2.22
$C_{36}H_{74}$	0.2830	0.3083	−0.6032	0.3167	0.35	1.94
Average deviation					0.51	2.74

Table 6
Correlations coefficients for calculating the influence parameters, its constant value for $T_r = 0.65$ and modeling results for n-alkanols

Fluid	$D \times 10^{16}$	$E \times 10^{16}$	$F \times 10^{16}$	$c/ab^{2/3} \times 10^{16}$ const	%AAD	
					σ (corr)	σ ($c/ab^{2/3} \times 10^{16}$ const)
CH_3OH	0.8476	−1.3824	0.7391	0.4519	0.04	7.70
C_2H_5OH	1.0544	−2.2174	1.7132	0.4889	0.04	8.60
C_3H_7OH	1.1401	−2.8386	2.4718	0.4466	0.07	5.75
C_4H_9OH	0.8650	−2.1548	1.8732	0.3344	0.20	7.40
$C_5H_{11}0H$	0.7366	−1.5314	1.1079	0.3235	0.02	8.10
$C_6H_{13}OH$	0.9373	−2.3260	2.0954	0.3773	0.53	10.09
$C_7H_{15}OH$	0.8293	−1.8311	1.4169	0.3638	0.30	10.85
$C_8H_{17}OH$	0.9553	−2.1822	1.7625	0.4037	0.47	10.65
$C_9H_{19}OH$	1.0431	−2.4854	1.9811	0.4132	0.39	12.32
$C_{10}H_{21}OH$	1.1957	−2.9749	2.3931	0.4465	0.65	13.61
$C_{11}H_{23}OH$	0.7684	−1.2776	0.7511	0.4112	0.09	7.84
$C_{12}H_{25}OH$	0.6523	−0.7458	0.1333	0.4058	0.27	8.17
$C_{13}H_{27}OH$	0.4330	0.0268	−0.4188	0.3929	0.71	3.14
$C_{14}H_{29}OH$	0.3258	0.3249	−0.6803	0.3566	1.09	2.65
$C_{15}H_{31}OH$	0.3170	0.4385	−0.8237	0.3703	0.85	2.57
$C_{16}H_{33}OH$	0.2924	0.4441	−0.7902	0.3519	1.08	2.75
$C_{17}H_{35}OH$	0.1847	0.7868	−1.0310	0.3347	1.03	3.31
$C_{18}H_{37}OH$	0.0653	1.4016	−1.8474	0.3283	0.69	3.48
$C_{19}H_{39}OH$	0.0669	1.4111	−1.8462	0.3331	0.62	3.61
$C_{20}H_{41}OH$	0.0626	1.4201	−1.8823	0.3275	0.83	3.55
Average deviation					0.50	6.81

of the surface tension data available and their accuracy, especially for the heavier members of the series.

Because of that, and following a previous work by the authors [44], a quadratic correlation is initially proposed for the variation of the influence parameter with reduced temperature (Eq. (14)):

$$\frac{c}{ab^{2/3}} = D + E \times (1 - T_r) + F \times (1 - T_r)^2 \qquad (14)$$

The correlation parameters D, E and F where regressed using Eq. (4) in the reduced temperature range $0.45 < T_r < 0.85$ for n-alkanes and n-alkanols and in the range $T_r > 0.43$ for fluoroalkanes, and are presented in Tables 5–7.

However, the dependence of the influence parameter with temperature far from the critical point is very weak and, as mentioned before, for the heavier n-alkanes and n-alkanols, data is only available in a short range of reduced temperatures, making the influence parameter almost constant. Because of this, calculations where also performed using the influence parameter at the reduced temperature of 0.65.

The results for the constant influence parameter and for the correlated coefficients of Eq. (14) are presented in Tables 5–7 for the different families evaluated in this work.

As for the CPA pure component parameters, the constant gradient theory influence parameters also seem to follow a trend with the van der Waals volume, as well as their correlation coefficients in Eq. (14). In fact, the values for the constant influence parameter of the n-alkanes and n-alkanols are very similar in the range $C_{10}–C_{20}$, and therefore an equal correlation for the variation of this parameter with the van der Waals volume can be proposed for these two families. The fitted quadratic correlations are presented in Table 8.

With these influence parameters, surface tensions were calculated as a function of temperature for the 30 n-alkanes, 20 n-alkanols and 7 n-perfluoroalkanes evaluated in this work. The comparison is performed against correlations of the available experimental data for each fluid in the reduced temperature range ($0.45 < T_r < 0.85$) in order to be able to evaluate both temperature effects and possible trends in the homologous series in the modeling results.

Tables 5–7 present the fluid average absolute deviations when using (i) the quadratic temperature dependency on reduced temperature and (ii) the constant influence parameters. As can be seen, it was possible to compute the surface tensions with a global aver-

age deviation of 0.5% for the three families when using Eq. (14) for the influence parameters. If these are made constant, the deviations increase, as expected, especially for n-alkanols, where the quadratic dependence is more evident as can be seen from the higher magnitude of the F values to be used in Eq. (14), as presented in Table 6. Still, the average global deviation is kept below 7%, which can be interesting for the cases where predictions may be required. Fu et al. studied pure n-alkanes from C1–C10 [79] with SAFT and from C1–C10, C20 and C22 with PC-SAFT [80] in both cases with a constant influence parameter. They reported an overall average deviation of 1.9% with PC-SAFT and 2.7% with SAFT. With a constant influence parameter, our average deviation was 2.7%, as reported in Table 5, but our range of n-alkanes C2–C36 and reduced temperature was considerably larger. Fu also studied 16 associating pure components using PC-SAFT [38]. Among these, there were n-alkanols between C1–C9. Deviations in terms of surface tensions (0.7–4.4%), using, this time, a linear temperature dependency for the influence parameter are higher than those presented here using Eq. (14), but lower than those obtained in this work using a constant influence parameter, thus showing the importance of using the right temperature dependency.

Pàmies [81] calculated surface tensions for some n-alkanes (C2–C20) and n-alkanols (C1–C8) with density gradient theory combined with soft-SAFT and constant influence parameters. Although from the graphical presentation a good description was obtained, no deviation is reported in order to compare with our results. Miqueu [45] calculated the deviations for n-alkanes from

Table 7
Correlations coefficients for calculating the influence parameters and modeling results for n-fluoroalkanes

Fluid	$D \times 10^{16}$	$E \times 10^{16}$	$F \times 10^{16}$	%AAD
				σ (corr)
C_3F_8	2.2151	−3.0122	1.7658	0.44
C_4F_{10}	0.9164	−1.1866	0.7642	0.18
C_5F_{12}	0.6707	−0.3453	0.0000	1.54
C_6F_{14}	0.7593	−0.7967	0.4601	0.62
C_7F_{16}	0.7943	−0.8387	0.3912	0.05
C_8F_{18}	0.7702	−1.1438	0.7734	0.09
C_9F_{20}	0.8094	−1.3234	1.1118	0.83
Average deviation				0.54

Table 8
Correlations for the variation of the constant value of the influence parameter and for the correlation coefficients in Eq. (14), with the van der Waals volume
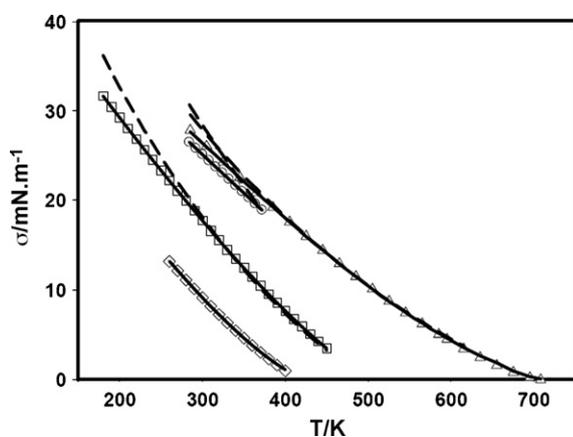
	n-Alkanes	n-Alkanols
$D \times 10^{16}$	$14.97V_{VDW}^2 - 8.24V_{VDW} + 1.26$	$-33.72V_{VDW}^2 + 3.47V_{VDW} + 0.89$
$E \times 10^{16}$	$-38.59V_{VDW}^2 + 20.27V_{VDW} - 1.81$	$146.34V_{VDW}^2 - 17.09V_{VDW} - 1.69$
$F \times 10^{16}$	$29.79V_{VDW}^2 - 15.73V_{VDW} + 0.77$	$-149.08V_{VDW}^2 + 18.07V_{VDW} + 1.19$
	n-FC	n-Alkanes/n-alkanols, $c/ab^{2/3} \times 10^{16}$ const
$D \times 10^{16}$	$363.75V_{VDW}^2 - 88.16V_{VDW} + 5.90$	$4.15V_{VDW}^2 - 2.63V_{VDW} + 0.70$
$E \times 10^{16}$	$-706.60V_{VDW}^2 + 162.56V_{VDW} - 9.83$	
$F \times 10^{16}$	$537.98V_{VDW}^2 - 119.28V_{VDW} + 6.82$	

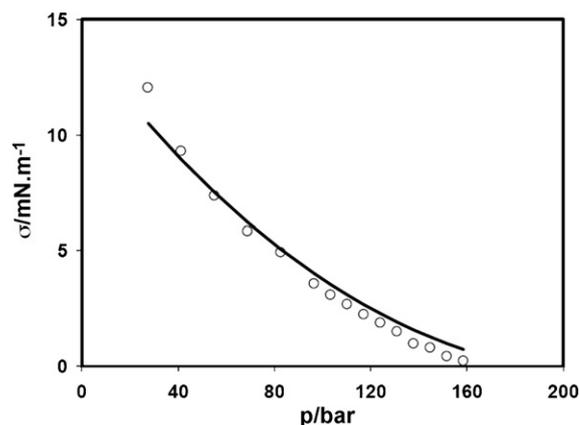C1–C16 using a volume-translated Peng-Robinson EoS. Deviations reported were within 0.7–2.5%.

Fig. 3 presents plots of surface tension as a function of temperature for different fluids. As can be seen, the trend with temperature is perfectly described by the proposed model, both for fluids from different families as well as short chain and long chain fluids, which indicate that the proposed model is an adequate tool for surface tension modeling.

As mentioned before, the combination of the gradient theory with the CPA EoS was also applied to mixtures of alkanes and alkanols following the algorithm described by Miqueu et al. [32]. Unfortunately not much data is available for mixtures of perfluoralkanes and therefore these were not studied. The gradient theory was used as a predictive method: setting the binary interaction coefficients to zero what allowed the use of the geometric mean combining rule for the influence parameters. The required data was collected from the compilation Landolt-Börnstein [82] for the ethane + nonane and the methanol + ethanol mixtures. For the methane + pentane mixture the data was collected from Amin et al. [83] and for the n-octane + 1-heptanol and n-octane + 1-octanol from Segade et al. [84]. Figs. 4–7 present plots of interfacial tensions as a function of temperature, pressure or composition for three of the four different mixtures studied.

It was possible to predict the surface tensions with a global average deviation of 43% for the methane + pentane mixture, of 2% for the ethane + nonane system, 1% for the methanol + ethanol mixture, 11% for 1-heptanol + n-octane and 7% for 1-octanol + n-octane. For the methane + pentane mixture the worst description occurred at the lower and higher pressures, as already found before by Miqueu et al. using a volume translated Peng-Robinson equation of state [28]. At this point it should also be noted that this system at the specified conditions has very low interfacial tensions, making the predictions more difficult. At this point, we should stress that CPA, with the parameters regressed from subcritical
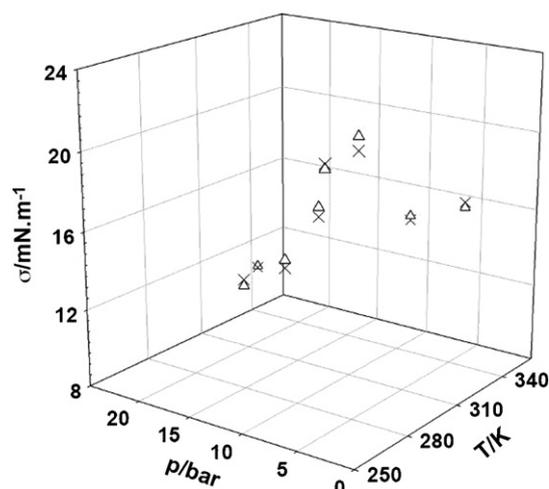

Fig. 4. Surface tension of the mixture methane + pentane at 310.95 K. Experimental (○), and gradient theory results (−).

data, cannot adequately describe critical points, so the larger deviations close to the critical point are certainly a consequence of that limitation.

Mixtures of alkanes and alkanols are frequently difficult to model with the approach proposed before: ($k_{ij} = 0$ in Eq. (5)). In fact, we tried to model other mixtures with lower alkanols and n-alkanes and some of the density profiles could not be calculated, avoiding the calculation of the surface tensions. In some of these mixtures a k_{ij} different from zero will have to be used, changing the solution of a set of algebraic equations to a set of differential equations for solving the density profiles.

Fig. 3. Surface tension. Experimental (□, C_6H_{14}; ○, $C_5H_{11}OH$; ◇, C_5F_{12}; △, $C_{15}H_{32}$) and gradient theory results ((−) using Eq. (14); (- - -) using a constant value for c_{ii}).

Fig. 5. Surface tension of the mixture ethane + nonane. Experimental (△), and gradient theory results (×).
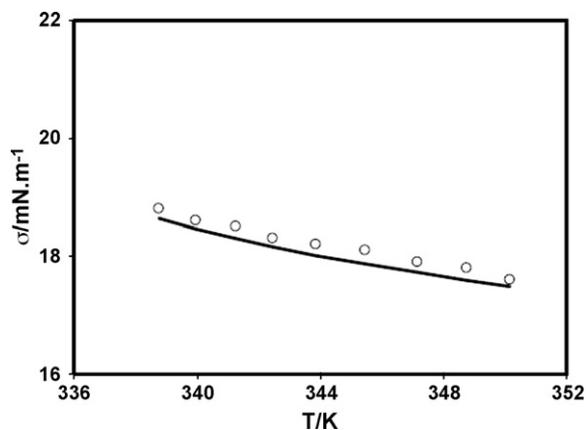
Fig. 6. Surface tension for the mixture methanol + ethanol. Experimental ($\bigcirc$), and gradient theory results (–).
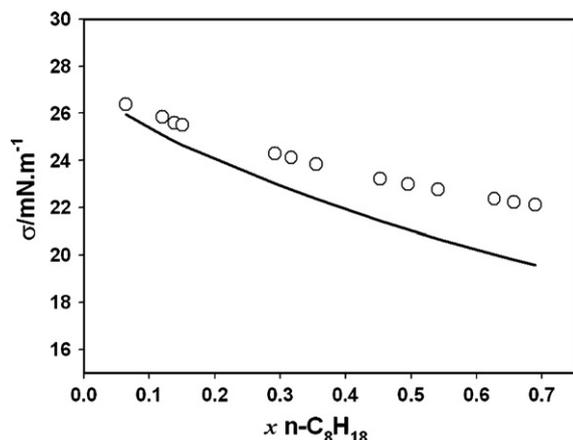

Fig. 7. Surface tension of *n*-octanol + *n*-octane mixture at 298.15 K. Experimental ($\bigcirc$) and gradient theory results (–).

4. Conclusions

In this work the coupling of the density gradient theory with the CPA EoS was applied to the description of surface tensions of homologue families of non-associating (*n*-alkanes and *n*-fluoroalkanes) and associating components (*n*-alkanols). CPA allowed the satisfactory computation of both liquid and vapor phase properties for the compounds selected with no need to perform any volume correction, as the parameters of the EoS were fitted on saturation pressures and liquid density data. These parameters showed to have a trend within the homologous series, and the correlations developed here allow the proposed approach to be used as a predictive tool.

The gradient theory with a quadratic correlation of the influence parameter in T_r allows very accurate estimations of surface tensions, with global average errors of 0.5% in the $0.45 < T_r < 0.85$ range.

For the heavier members of the *n*-alkane and *n*-alkanol families, the assumption of a constant value for the influence parameter seemed to be more appropriate, but this also resulted in higher average deviations.

The broad surface tension database that was evaluated in this work (57 fluids from three different families) ensures that the proposed model can adequately be used for modeling surface tensions in a wide temperature range. In addition, the gradient theory can be used as a predictive method allowing estimations of surface tensions of some mixtures of hydrocarbons + hydrocarbons, alkanols + alkanols and hydrocarbons + long chain alkanols with a good agreement with the available experimental data.

List of symbols
a	energy parameter in the physical term
a_0, c_1	parameters for calculating a
b	co-volume
c	influence parameter
D, E, F	correlation coefficients for the influence parameter
f_0	Helmholtz free energy density
g	radial distribution function
k	binary interaction coefficient
n	mole number, mole density
N	mixture reference component
p	vapor pressure
R	gas constant
T	temperature
x	mole fraction
X_{Ai}	mole fraction of component i not bonded at site A
Z	compressibility factor

Greek letters
β	association volume
ε	association energy
σ	surface tension
Ω	grand thermodynamic potential
η	reduced fluid density
μ	chemical potential
ρ	mole density
Δ	association strength

Subscripts
c	critical
i, j	pure component indexes
liq.	liquid
r	reduced

Superscripts
assoc.	association
phys.	physical

Appendix A. Helmholtz energy density and chemical potential of the CPA EoS (SRK cubic term)

The CPA Helmholtz energy density is given by:

$$f_0 = \frac{A}{V} = -\rho RT - \rho RT \ln\left(\frac{p}{RT}\right) + RT\sum_i \rho_i \ln(\rho_i) - \frac{a\rho}{b}\ln(1 + b\rho)$$

$$-\rho RT \ln(1 - b\rho) + RT\sum_i \rho_i \sum_{A_i}\left[\ln(X_{Ai}) - \frac{X_{Ai}}{2} + \frac{1}{2}\right]$$

and the CPA chemical potential by:

$$\mu_i = -RT \ln(1-b\rho) - \frac{2}{b}\ln(1+b\rho)\sum_j x_j a_{ij} + \left\{ \frac{RT\rho}{1-b\rho} + \frac{a}{b^2}\ln(1+b\rho) \right.$$

$$\left. - \frac{a\rho}{b(1+b\rho)} \right\} \times \left(2\sum_j x_j b_{ij} - b \right)$$

$$+ RT \left\{ \sum_{A_i} \ln(X_{Ai}) - \frac{1}{2}\sum_j x_j \sum_{Aj}(1-X_{Aj})\frac{\partial \ln g}{\partial n_i} \right\}.$$

References

[1] H.T. Kennedy, E.T. Guerrero, Trans. Am. Inst. Mining Metall. Eng. 201 (1954) 124–131.
[2] M. Gonuguntla, A. Sharma, J. Sarkar, S.A. Subramanian, M. Ghosh, V. Shenoy, Phys. Rev. Lett. 97 (2006) 18304.
[3] D.T. Wasan, A.D. Nikolov, L.A. Lobo, K. Koczo, D.A. Edwards, Prog. Surf. Sci. 39 (1992) 119–154.
[4] C. Cramer, P. Fischer, E.J. Windhab, Chem. Eng. Sci. 59 (2004) 3045–3058.
[5] T. Karbowiak, F. Debeaufort, A. Voilley, Crit. Rev. Food Sci. 46 (2006) 391–407.
[6] J. Straub, Exp. Therm. Fluid Sci. 9 (1994) 253–273.
[7] D.B. MacLeod, Trans. Faraday Soc. 19 (1923) 38–41.
[8] E.A. Guggenheim, J. Chem. Phys. 13 (1945) 253–261.
[9] Y.X. Zuo, E.H. Stenby, Can. J. Chem. Eng. 75 (1997) 1130–1137.
[10] A.J. Queimada, L.I. Rolo, A.I. Caco, I.M. Marrucho, E.H. Stenby, J.A.P. Coutinho, Fuel 85 (2006) 874–877.
[11] A.J. Queimada, A.I. Caco, I.M. Marrucho, J.A.P. Coutinho, J. Chem. Eng. Data 50 (2005) 1043–1046.
[12] P.H. Winterfeld, L.E. Scriven, H.T. Davis, AIChE J. 24 (1978) 1010–1014.
[13] L.A. Girifalco, R.J. Good, J. Phys. Chem. 61 (1957) 904–909.
[14] F.M. Fowkes, J. Phys. Chem. 66 (1962) 1863–1866.
[15] S. Toxvaerd, J. Chem. Phys. 57 (1972) 4092–4097.
[16] S. Nordholm, M. Johnson, B.C. Freasier, Aust. J. Chem. 33 (1980) 2139–2150.
[17] R. Evans, Adv. Phys. 28 (1979) 143–200.
[18] B.S. Almeida, M.M.T. Dagama, J. Phys. Chem. 93 (1989) 4132–4138.
[19] V. Bongiorno, H.T. Davis, Phys. Rev. A 12 (1975) 2213–2224.
[20] J.S. Rowlinson, J. Stat. Phys. 20 (1979) 197–244.
[21] J.W. Cahn, J.E. Hilliard, J. Chem. Phys. 28 (1958) 258–267.
[22] S.B. Kiselev, J.F. Ely, J. Chem. Phys. 119 (2003) 8645–8662.
[23] C. Panayiotou, J. Colloid Interface Sci. 267 (2003) 418–428.
[24] J.F. Lu, D. Fu, J.C. Liu, Y.G. Li, Mol. Simulat. 29 (2003) 809–815.
[25] B.S. Carey, L.E. Scriven, H.T. Davis, AIChE J. 26 (1980) 705–711.
[26] P.M.W. Cornelisse, C.J. Peters, J.D. Arons, Fluid Phase Equilib. 82 (1993) 119–129.
[27] P.M.W. Cornelisse, C.J. Peters, J.D. Arons, Mol. Phys. 80 (1993) 941–955.
[28] C. Miqueu, B. Mendiboure, C. Graciaa, J. Lachaise, Fluid Phase Equilib. 218 (2004) 189–203.
[29] M. Sahimi, B.N. Taylor, J. Chem. Phys. 95 (1991) 6749–6761.
[30] Y.X. Zuo, E.H. Stenby, J. Colloid Interface Sci. 182 (1996) 126–132.
[31] C. Miqueu, B. Mendiboure, A. Graciaa, J. Lachaise, Fluid Phase Equilib. 207 (2003) 225–246.
[32] C. Miqueu, B. Mendiboure, A. Graciaa, J. Lachaise, Ind. Eng. Chem. Res. 44 (2005) 3321–3329.
[33] H. Kahl, S. Enders, Fluid Phase Equilib. 172 (2000) 27–42.
[34] A. Mejia, H. Segura, L.F. Vega, J. Wisniak, Fluid Phase Equilib. 227 (2005) 225–238.
[35] A. Mejia, H. Segura, J. Wisniak, I. Polishuk, J. Phase Equilib. Diff. 26 (2005) 215–224.
[36] P.M.W. Cornelisse, M. Wijtkamp, C.J. Peters, J. de Swaan Arons, Fluid Phase Equilib. 151 (1998) 633–640.
[37] C. Panayiotou, Langmuir 18 (2002) 8841–8853.
[38] D. Fu, Ind. Eng. Chem. Res. 46 (2007) 7378–7383.
[39] I.V. Yakoumis, G.M. Kontogeorgis, E.C. Voutsas, E.M. Hendriks, D.P. Tassios, Ind. Eng. Chem. Res. 37 (1998) 4175–4182.
[40] G.K. Folas, G.M. Kontogeorgis, M.L. Michelsen, E.H. Stenby, Ind. Eng. Chem. Res. 45 (2006) 1527–1538.
[41] G.K. Folas, J. Gabrielsen, M.L. Michelsen, E.H. Stenby, G.M. Kontogeorgis, Ind. Eng. Chem. Res. 44 (2005) 3823–3833.
[42] S.O. Derawi, G.M. Kontogeorgis, M.L. Michelsen, E.H. Stenby, Ind. Eng. Chem. Res. 42 (2003) 1470–1477.
[43] M.B. Oliveira, M.G. Freire, I.M. Marrucho, G.M. Kontogeorgis, A.J. Queimada, J.A.P. Coutinho, Ind. Eng. Chem. Res. 46 (2007) 1415–1420.
[44] A.J. Queimada, C. Miqueu, I.M. Marrucho, G.M. Kontogeorgis, J.A.P. Coutinho, Fluid Phase Equilib. 228 (2005) 479–485.
[45] C. Miqueu, Modélisation à Température et Pression Élevées de la Tension Superficielle de Composants des Fluides Pétroliers et de Leurs Mélanges Synthétiques ou Réels, Ph.D. Thesis, Université de Pau et des Pays de L'Adour, Pau, France, 2001.
[46] G.M. Kontogeorgis, E.C. Voutsas, I.V. Yakoumis, D.P. Tassios, Ind. Eng. Chem. Res. 35 (1996) 4310–4318.
[47] E.C. Voutsas, G.C. Boulougouris, I.G. Economou, D.P. Tassios, Ind. Eng. Chem. Res. 39 (2000) 797–804.
[48] G.M. Kontogeorgis, I.V. Yakoumis, H. Meijer, E. Hendriks, T. Moorwood, Fluid Phase Equilib. 160 (1999) 201–209.
[49] J.Z. Wu, J.M. Prausnitz, Ind. Eng. Chem. Res. 37 (1998) 1634–1643.
[50] M.L. Michelsen, E.M. Hendriks, Fluid Phase Equilib. 180 (2001) 165–174.
[51] S.H. Huang, M. Radosz, Eng. Chem. Res. 29 (1990) 2284–2294.
[52] NIST Chemistry WebBook, http://www.webbook.nist.gov/chemistry/fluid/.
[53] DIPPR, Thermophysical Properties Database, 1998.
[54] R.D. Chirico, A. Nguyen, W.V. Steele, M.M. Strube, J. Chem. Eng. Data 34 (1989) 149–156.
[55] A.P. Kudchadk, B.J. Zwolinsk, J. Chem. Eng. Data 11 (1966) 253–255.
[56] D.L. Morgan, R. Kobayashi, Fluid Phase Equilib. 97 (1994) 211–242.
[57] V. Piacente, D. Fontana, P. Scardala, J. Chem. Eng. Data 39 (1994) 231–237.
[58] D. Ambrose, J. Chem. Thermodyn. 13 (1981) 1161–1167.
[59] D. Ambrose, J.H. Ellender, J. Chem. Thermodyn. 13 (1981) 901–902.
[60] J.F. Counsell, J.H.S. Green, J.L. Hales, J.F. Martin, Trans. Faraday Soc. 61 (1965) 212–218.
[61] G.A. Crowder, Z.L. Taylor, T.M. Reed, J.A. Young, J. Chem. Eng. Data 12 (1967) 481–485.
[62] A.M.A. Dias, A.I. Caco, J.A.P. Coutinho, L.M.N.B.F. Santos, M.M. Pineiro, L.F. Vega, M.F.C. Gomes, I.M. Marrucho, Fluid Phase Equilib. 225 (2004) 39–47.
[63] A.M.A. Dias, C.M.B. Goncalves, A.I. Caco, L.M.N.B.F. Santos, M.M. Pineiro, L.F. Vega, J.A.P. Coutinho, I.M. Marrucho, J. Chem. Eng. Data 50 (2005) 1328–1333.
[64] A.M.A. Dias, C.M.B. Goncalves, J.L. Legido, J.A.P. Coutinho, I.M. Marrucho, Fluid Phase Equilib. 238 (2005) 7–12.
[65] D.R. Douslin, A. Osborn, J. Sci. Instrum. 42 (1965) 369–373.
[66] R.D. Dunlap, C.J. Murphy, R.G. Bedford, J. Am. Chem. Soc. 80 (1958) 83–85.
[67] T.J.V. Findlay, J. Chem. Eng. Data 14 (1969) 229–231.
[68] J.L. Hales, R. Townsend, J. Chem. Thermodyn. 6 (1974) 111–116.
[69] R.N. Haszeldine, F. Smith, J. Chem. Soc. (1951) 603–608.
[70] R.P. Kennan, G.L. Pollack, J. Chem. Phys. 89 (1988) 517–521.
[71] A. Kreglewski, B Acad. Pol. Sci.-Chim. 10 (1962) 629.
[72] G.D. Oliver, S. Blumkin, C.W. Cunningham, J. Am. Chem. Soc. 73 (1951) 5722–5725.
[73] W.V. Steele, R.D. Chirico, S.E. Knipmeyer, A. Nguyen, J. Chem. Eng. Data 42 (1997) 1021–1036.
[74] V.E. Stiles, G.H. Cady, J. Am. Chem. Soc. 74 (1952) 3771–3773.
[75] I.V. Yakoumis, G.M. Kontogeorgis, E.C. Voutsas, D.P. Tassios, Fluid Phase Equilib. 130 (1997) 31–47.
[76] E.C. Voutsas, G.M. Kontogeorgis, I.V. Yakoumis, D.P. Tassios, Fluid Phase Equilib. 132 (1997) 61–75.
[77] G.M. Kontogeorgis, M.L. Michelsen, G.K. Folas, S. Derawi, N. von Solms, E.H. Stenby, Ind. Eng. Chem. Res. 45 (2006) 4855–4868.
[78] H. Lin, Y.Y. Duan, Q. Min, Fluid Phase Equilib. 254 (2007) 75–90.
[79] D. Fu, J. Phys. Chem. B 110 (2006) 19575–19581.
[80] D. Fu, X.S. Li, S.M. Yan, T. Liao, Ind. Eng. Chem. Res. 45 (2006) 8199–8206.
[81] J.C. Pàmies, Bulk and Interfacial Properties of Chain Fluids: A Molecular Modelling Approach, Ph.D. Thesis, Universitat Rovira i Virgili, Tarragona, Spain, 2003.
[82] C. Wohlfarth, B. Wohlfarth, Surface Tension of Pure Liquids and Binary Liquid Mixtures, in: M.D. Lechner (ed.), Landolt-Börnstein Numerical Data and Functional Relationships in Science and Technology, Group IV: Physical Chemistry, vol. 16, Springer, Berlin, 1997.
[83] R. Amin, T.N. Smith, Fluid Phase Equilib. 142 (1998) 231–241.
[84] L. Segade, J.J. de Llano, M. Dominguez-Perez, O. Cabeza, M. Cabanas, E. Jimenez, J. Chem. Eng. Data 48 (2003) 1251–1255.